Electronic Research Archive

https://www.aimspress.com/journal/era

ERA, 34(9): 5968–5992.
DOI: 10.3934/era.2026264
Received: 08 April 2026
Revised: 01 June 2026
Accepted: 09 June 2026
Published: 13 July 2026

Research article

Analytical and dynamical investigations of the Kaup–Kupershmidt model via two innovative integrability architectures

Saud Owyed*

Department of Mathematics, College of Sciences, University of Bisha, Bisha 61922, Saudi Arabia

* **Correspondence:** Email: saalgamdi@ub.edu.sa.

Abstract: This study focused on the modified F-expansion method and the $\frac{G'}{bG'+G+a}$-expansion method to find exact solutions to the $(1+1)-$dimensional Kaup–Kupershmidt (KK) equation, an important nonlinear model that incorporates both dispersive effects and higher-order nonlinearity. By applying these analytical techniques, several classes of exact solutions, including periodic, bright, and singular soliton solutions, were successfully obtained. The graphical representation of these solutions was evaluated by creating two-dimensional, three-dimensional, and contour plots for each solution type to explore the wide range of dynamic behaviors associated with these solutions. Additionally, modulation instability for the equation was determined with linear stability analysis. Observing the outcomes, it is clearly evident that the suggested methods are significant mathematical tools to solve nonlinear partial differential equations arising in various areas of applied mathematics and physics. The novelty of the work lies in the combined application of the $\frac{G'}{bG'+G+a}$-expansion and modified F-expansion methods to the KK equation, providing broader classes of exact solutions and deeper insight into the equation's nonlinear dynamics beyond earlier studies in the literature.

Keywords: optical soliton solutions; analytical techniques; Kaup–Kupershmidt model; $\frac{G'}{bG'+G+a}$-expansion method; wave profile analysis; constraints; modified F-expansion method

1. Introduction

Nonlinear evolution equations (NLEEs) are of central importance because they are extensively employed to model a broad range of physical phenomena encountered in science and engineering [1, 2]. The concept of solitons and the study of nonlinear wave equations have contributed to many developments in the field of applied sciences [3]. Solitons as well as solitary waves arise across a wide range of settings, for instance in biological models, optical communication systems, water shallow waves, Bose–Einstein condensates, and deep water wave dynamics [4, 5].

In the 1800s, John Scott Russell, a naval architect and Scottish civil engineer, first saw these waves [6].

After making this first discovery, he described the phenomenon as "the great wave of translation." A soliton is a special kind of wave solution that moves at a constant speed without losing its shape in a nonlinear medium [7]. Optical solitons [8] are a big part of soliton theory because they are used in many ways in communication and information technologies.

In recent years, many researchers have found the analytical ways to study the NLEEs, one of the most interesting and exciting area of scientific research. As a result, numerous novel techniques have been developed including the modified generalized Riccati equation mapping method [9], the sine-Gordon expansion method [10], the modified simple equation method [11], the new extended direct algebraic method [12], expansions of the new generalized (G'/G)-method [13], the new $\phi6$ model [14], the modified Khater method [15], the new auxiliary equation method [16], the Hirota's bilinear method [17], the $exp(-\phi(\xi))$-expansion method [18], the inverse scattering method [19], the generalized Kudryashov method [20], the sine-cosine method [21], Lie group methods [22], and other approaches. New studies for nonlinear dispersive wave models have explain the cruciality of analytical structures, instability analysis, bifurcation analysis, and graphical illustrations to comprehend complex wave dynamics. Specially, the combined need of exact, approximation, and stability approaches has been given deeper understanding for wave propagation, parameteric sensitivity, and existence of closed wave families in nonlinear physical models. The generalized (2 + 1)-dimensional KK equation is given by

$$a_1u_t + a_2u_{5x} + a_3uu_{xxx} + a_4u_xu_{xx} + a_5u^2u_x + a_6u_{xxy} + a_7\partial_x^{-1}u_{yy} + a_8uu_y + a_9u_x\partial_x^{-1}u_y = 0, \tag{1.1}$$

where $(u = u(x, y, t))$ represents the wave function, while the constraints $(a_i, (i = 1, 2, \dots, 9))$ denote strengths of temporal fraction, higher-order dispersion, nonlinear interaction, and transverse perturbation effects, respectively. By selecting right parametric values, the generalized model converts to the very specific (2 + 1)- dimensional KK model [23]:

$$9u_t + u_{5x} + 15uu_{xxx} + \frac{75}{2}u_xu_{xx} + 45u^2u_x + 5\sigma u_{xxy} - 5\sigma\partial_x^{-1}u_{yy} + 15\sigma uu_y + 15\sigma u_x\partial_x^{-1}u_y = 0. \tag{1.2}$$

Here, the fifth-order derivative term represents higher-order dispersion effects, the nonlinear terms describe wave interaction mechanisms, and the y-dependent terms characterize the influence of transverse perturbations in the propagation dynamics. In the present study, the normalized parameter value $\sigma^2 = 1$ is adopted, which is commonly used in the literature to simplify the mathematical analysis while preserving the essential nonlinear, dispersive, and transverse characteristics of the KK model. Different values of σ^2 modify the strength of the transverse perturbation effects and may influence the amplitude, width, and propagation behavior of the resulting wave structures. The remaining parameter values are selected according to the analytical constraints of the employed analytical methods and to obtain physically meaningful localized wave profiles. Furthermore, ∂_x^{-1} denotes the inverse differential operator, defined by $\partial_x^{-1} = \int dx$. When $u_y = 0$, one obtains the the classical (1+1)-dimensional KK equation [24]:

$$9u_t + u_{5x} + 15uu_{xxx} + \frac{75}{2}u_xu_{xx} + 45u^2u_x = 0. \tag{1.3}$$

The KK equation is an important higher-order nonlinear evolution model that arises along the study for nonlinear wave propagation and integrable systems in mathematical physics. It consists of significant utilizations in fluid dynamics, wave theory, shallow water, plasma physics, and nonlinear dispersive media, where it is used to describe the interaction and propagation of nonlinear solitary waves. Because of rich mathematical structure or physical importance, the equation has attracted attention when investigating exact traveling wave solutions and nonlinear wave phenomena. Special polynomial and vortex solutions related to the KK and Sawada–Kotera equations were examined by Demina and Kudryashov [25]. Akbulut et al. [26] solved the fifth-order (1+1)-dimensional Kdv equation analytically and derived conservation rules. Furthermore, Inc et al. [27] utilized the new sub-equation method for constructing conformable fractional solutions, whereas Iqbal et al. [28] used special integral transform techniques to analyze the fractional-order form of the KK equation. Moreover, Kim et al. [29] established Liouville correspondences between the KK and Degasperis–Procesi hierarchies, which demonstrated the intimate relationships among integrable systems. Collectively, these investigations underscore the equation's richness, generality, and significance in the mathematical study of nonlinear phenomena.

The (1 + 1)-dimensional KK model has been extensively investigated in literature for its essential applications in nonlinear wave propagation, fluid dynamics, and mathematical physics. Different exact techniques, including the Hirota bilinear method [30], inverse scattering transform [31], tanh-function method [32], Jacobi elliptic function approaches [33], Exp-function method [34], (G'/G)-expansion method [35], and Bäcklund transformation [36], have been employed to derive exact solutions of the KK equation. However, most of the previous studies mainly focused on standard forms of solution methods and produced limited classes of periodic wave solutions and solitary wave solutions. In particular, the classical (G'/G)-expansion method often generates solutions that are equivalent to previously reported hyperbolic or trigonometric forms. Recent studies have further explored analytical and semi-analytical techniques for solving nonlinear evolution equations, using different expansion and transformation methods [37, 38]. In particular, several works have reported new exact soliton solutions and their physical behaviors, demonstrating the richness of solution structures in such nonlinear models. In contrast, the present study applies the generalized $(G'/(bG' + G + a))$-expansion method together with the modified F-expansion method to derive more comprehensive exact solutions of the KK equation. The inclusion of additional free parameters in the $(G'/(bG' + G + a))$-expansion method increases the flexibility of the solution structure and yields wider families of trigonometric, rational solutions, and hyperbolic solutions, whereas the modified F-expansion technique provides abundant periodic wave solutions and Jacobi elliptic solutions in a unified framework. Therefore, compared with earlier works, the present study extends the existing literature by constructing richer and more generalized exact traveling wave solutions and by demonstrating the effectiveness of these improved analytical techniques for higher-order NLEEs. In this current work, our main concern is to explore some new and general exact traveling wave solutions of the KK equation, with the help of the modified F-expansion method (MFEM) [39] and the $\frac{G'}{bG'+G+a}$-expansion technique [40]. Motivated by the requirement for efficient and reliable analytical methods, the present paper applies the modified F-expansion method and the $\frac{G'}{bG'+G+a}$-expansion technique for constructing novel exact solutions of governing model. These approaches provide systematic methodology for deriving diverse structures, including bright, periodic, or singular soliton solutions. Also, the graphical investigation with modulation instability analysis [41, 42] offers deeper insight into the dynamical behavior and stability properties of the obtained solutions, which may contribute to future studies in nonlinear science and applied mathematics. The MFEM represents an extended form of the conventional F-expansion approach. In the modified form, more parameters or transformation functions are added to the method in order to make it more flexible and applicable to a wider range of nonlinear equations. By eliminating the need for time-intensive bilinear transformations and intricate symbolic computations, these techniques provide an easier method for obtaining solutions that is more systematically structured, and can produce a wider range of exact solutions, such as rational, trigonometric, hyperbolic, and mixed-type solitons. This adaptability strengthens the model's analysis by allowing exploration of a broader range of parameter regimes while helping to detect wave behavior which may not be visible through other methods. These methods provide a way of solving problems and may help one understand more about the behavior of waves depending on the physical situation, particularly in dispersive media. Moreover, fractional extensions for integrable equations have been shown to extract richer solitons compared with classical integer-order models. Therefore, extending the suggested model into the fractional-order equation may supply deeper comprehension in memory dependent nonlinear propagation and be known as a crucial future direction of research [43–45].

The remainder of this paper is organized as follows: Section 2 presents the MFEM and its implementation. In Section 3, we describe the $\frac{G'}{bG'+G+a}$ method and apply it to the governing model. Section 4 provides the physical interpretation of the obtained results. Section 5 discusses the modulation instability of the given equation, while Section 6 discusses novelty of the paper. Section 7 concludes the paper with final remarks.

2. Modified F-expansion technique

Step 1. In this step, the traveling wave transformation is applied to obtain the nonlinear ordinary differential equation (NODE). Consider the given nonlinear partial differential equation (NLPDE):

$$G(u, u_x, u_{xx}, u_t, u_{xt}, \dots) = 0. \tag{2.1}$$

The subscripts in Eq (2.1) represent the partial derivative of u with respect to x and t. The corresponding expressions for the wave solution and the transformation are given as follows:

$$u(x, t) = U(\theta),\ \theta = x + ct. \tag{2.2}$$

The parameter c in Eq (2.2) denotes a real constant whose value is to be determined. By inserting Eq (2.2) into Eq (2.1), one obtains the following NODE:

$$M(U(\theta), U'(\theta), U''(\theta), U^2(\theta)U''(\theta), \dots) = 0, \tag{2.3}$$

where M is a polynomial in $U(\theta)$.

The proposed formulation provides a general analytical framework before it is specialized to the considered KK equation.

Step 2. We suppose that Eq (2.3) admits a solution that can be expressed in the following series form:

$$U(\theta) = \sum_{j=-n}^{n} A_j E^j(\theta). \tag{2.4}$$

In Eq (2.4), $A_{-n}, \dots, A_0, \dots, A_n$ are real constants that will be found later, where A_{-n} and A_n are not allowed to vanish simultaneously. The integer n denotes the balancing term, determined via the homogeneous balance principle by equating the highest degree of nonlinear terms and the orders of the highest derivative in Eq (2.3).

The function $E(\theta)$ satisfies the following differential equation (DE):

$$\frac{dE(\theta)}{d\theta} = T_2E^2(\theta) + T_1E(\theta) + T_0, \qquad T_2 \neq 0, \tag{2.5}$$

where T_0, T_1, and T_2 are provided in Table 1.
Step 3. Upon inserting Eq (2.4) and its corresponding derivatives into Eq (2.3), together with Eq (2.5), one obtains a polynomial expression in terms of $E(\theta)$. Setting the coefficients of each power of $E(\theta)$ equal to zero produces a system of algebraic equations for the unknown constants $A_{-n}, \ldots, A_n, T_0, T_1, T_2$, and c.
Step 4. Solving the above system provides several possible solution sets. Combining the suitable set with Eqs (2.2) and (2.4) gives the corresponding solution of the NLPDE in Eq (2.1).
The solution forms listed in Table 1 satisfy the auxiliary Riccati-type equation given in Eq (2.5) under the corresponding parameter values of T_0, T_1, and T_2. Similar auxiliary forms have also been reported in previous studies [39]. The expressions were further verified symbolically during the derivation procedure.

Table 1. Relationship between the values of T_0, T_1, T_2 and the corresponding forms of $E(\theta)$ in Eq (2.5).

Cases	T_0	T_1	T_2	$E(\theta)$
1	0	1	-1	$\frac{1}{2} + \frac{1}{2}\tanh(\theta/2)$
2	0	-1	1	$\frac{1}{2} - \frac{1}{2}\coth(\theta/2)$
3	$1/2$	0	$-1/2$	$\tanh(\theta) \mp i\,\mathrm{sech}(\theta), \coth(\theta) \mp \mathrm{csch}(\theta)$
4	1	0	-1	$\tanh(\theta),\ \coth(\theta)$
5	$1/2$	0	$1/2$	$\tan(\theta) + \mathrm{sech}(\theta), \mathrm{csch}(\theta) - \cot(\theta)$
6	$-1/2$	0	$-1/2$	$\csc(\theta) + \cot(\theta),\ \sec(\theta) - \tan(\theta)$
7	1	0	1	$\tan(\theta),\ \cot(\theta)$
8	-1	0	-1	$\tan(\theta),\ \cot(\theta)$
9	Arbitrary constant	$\neq 0$	0	$(e^{S\theta} - R)/S$, where S and R are real constants

2.1. Application of modified F-expansion method

Consider the following wave transformation:

$$u(x,t) = U(\theta), \theta = x + ct. \tag{2.6}$$

The expression $\theta = x + ct$ is mathematically equal to the more commonly used form, i.e., $\theta = x - ct$, distinct only by the sign of the propagation parameter c. Here, c has been treated as an algebraic wave speed parametric value occurring from the traveling wave transformation; therefore, the sign convention has no affect on the correctness of the extracted solutions, given it is used continuously throughout the study.

$$9c\left(\frac{dU}{d\theta}\right) + \frac{d^5U}{d\theta^5} + 15U\left(\frac{d^3U}{d\theta^3}\right) + \frac{75}{2}\left(\frac{dU}{d\theta}\right)\left(\frac{d^2U}{d\theta^2}\right) + 45U^2\left(\frac{dU}{d\theta}\right) = 0. \tag{2.7}$$

Additionally, the governing model has been carefully rechecked to make sure there is consistency among terms with nonlinear derivatives appearing in this equation and in the reduced (1 + 1)-dimensional equation. Specifically, the terms that that have a product of derivatives are keenly written in the reduced form as $U'U''$, respectively, to the u_xu_{xx} contribution after reduction.

The balancing term, $n = 2$, is obtained by using the homogeneous balance principle. Thus, Eq (2.4) takes on the following form:

$$U = A_{-2}E^{-2} + A_{-1}E^{-1} + A_0 + A_1E + A_2E^2, \tag{2.8}$$

where U satisfies the relation given in Eq (2.5). The combination of Eq (2.8) with Eqs (2.7) and (2.5) yields the following system:

$$[E(\theta)]^{-7}: \ -720T_0^5A_{-2} - 810T_0^3A_{-2}^2 - 90T_0A_{-2}^3 = 0,$$

$$\begin{aligned}[E(\theta)]^{-6}: \ & -2400A_{-2}T_0^4T_1 - 120\mathrm{A}_{-1}T_0^5 - 2010A_{-2}^2T_0^2T_1 - 825A_{-2}\mathrm{A}_{-1}T_0^3 - 90A_{-2}^3T_1 \\ & - 225A_{-2}^2\mathrm{A}_{-1}T_0 = 0,\end{aligned}$$

$$\begin{aligned}[E(\theta)]^{-5}: \ & - 224A_{-2}T_0^4T_2 - 400A_{-2}T_0^3T_1^2 - 48A_{-1}T_0^4T_1 - 220A_{-2}^2T_0^2T_2 - 216A_{-2}^2T_0T_1^2 \\ & - 262A_{-2}A_{-1}T_0^2T_1 - 48A_{-2}A_0T_0^3 - 22A_{-1}^2T_0^3 - 12A_{-2}^3T_2 - 56A_{-2}^2A_{-1}T_1 \\ & - 24A_{-2}^2A_0T_0 - 24A_{-2}A_{-1}^2T_0 - 6A_{-1}^3T_0 - 56A_{-2}^2T_1^3 - 36A_{-2}A_{-1}A_0T_0 \\ & - 108A_{-2}A_0T_0^2T_1 - 200A_{-2}A_{-1}T_0T_1^2 - 206A_{-2}A_{-1}T_0^2T_2 - 344A_{-2}^2T_0T_1T_2 \\ & - 18A_{-2}^2A_1T_0 - 528A_{-2}T_0^3T_1T_2 - 24A_{-2}A_{-1}^2T_1 - 24A_{-2}^2A_0T_1 - 30A_{-2}^2A_{-1}T_2 \\ & - 12A_{-1}A_0T_0^3 - 49A_{-1}^2T_0^2T_1 - 18A_{-2}A_1T_0^3 - 52A_{-1}T_0^3T_1^2 - 32A_{-1}T_0^4T_2 \\ & - 228A_{-2}T_0^2T_1^3 = 0,\end{aligned}$$

$$\begin{aligned}[E(\theta)]^{-4}: \ & - 45\mathrm{A}_{-1}{}^3T_0 - 420A_{-2}^2T_1^3 - 270A_{-2}\mathrm{A}_{-1}A_0T_0 - 810A_{-2}A_0T_0^2T_1 - 1500A_{-2}\mathrm{A}_{-1}T_0T_1^2 \\ & - 1545A_{-2}\mathrm{A}_{-1}T_0^2T_2 - 2580A_{-2}^2T_0T_1T_2 - 135A_{-2}^2A_1T_0 - 3960A_{-2}T_0^3T_1T_2 \\ & - 180A_{-2}\mathrm{A}_{-1}{}^2T_1 - 180A_{-2}^2A_0T_1 - 225A_{-2}^2\mathrm{A}_{-1}T_2 - 90\mathrm{A}_{-1}A_0T_0^3 - \frac{735}{2}\mathrm{A}_{-1}{}^2T_0^2T_1 \\ & - 135A_{-2}A_1T_0^3 - 390\mathrm{A}_{-1}T_0^3T_1^2 - 240\mathrm{A}_{-1}T_0^4T_2 - 1710A_{-2}T_0^2T_1^3 = 0,\end{aligned}$$

$$\begin{aligned}[E(\theta)]^{-3}: \ & - 1232A_{-2}T_0^3T_2^2 - 3104A_{-2}T_0^2T_1^2T_2 - 422A_{-2}T_0T_1^4 - 480A_{-1}T_0^3T_1T_2 \\ & - 180A_{-1}T_0^2T_1^3 - 990A_{-2}^2T_0T_2^2 - 960A_{-2}^2T_1^2T_2 - 2250A_{-2}A_{-1}T_0T_1T_2 \\ & - 360A_{-2}A_{-1}T_1^3 - 600A_{-2}A_0T_0^2T_2 - 570A_{-2}A_0T_0T_1^2 - 285A_{-2}A_1T_0^2T_1 \\ & - 60A_{-2}A_2T_0^3 - 270A_{-1}^2T_0^2T_2 - 255A_{-1}^2T_0T_1^2 - 180A_{-1}A_0T_0^2T_1 - 15A_{-1}A_1T_0^3 \\ & - 180A_{-2}^2A_0T_2 - 135A_{-2}^2A_1T_1 - 90A_{-2}^2A_2T_0 - 180A_{-2}A_{-1}^2T_2 \\ & - 270A_{-2}A_{-1}A_0T_1 - 180A_{-2}A_{-1}A_1T_0 - 90A_{-2}A_0^2T_0 - 45A_{-1}^3T_1 - 90A_{-1}^2A_0T_0 \\ & - 18A_{-2}cT_0 = 0,\end{aligned}$$

$$
\begin{aligned}
[E(\theta)]^{-2}:\ & -180A_{-2}A_1T_0T_1^2-195A_{-2}A_1T_0^2T_2-750A_{-2}A_{-1}T_1^2T_2-795A_{-2}A_{-1}T_0T_2^2\\
&-292A_{-1}T_0^2T_1^2T_2-884A_{-2}T_0T_1^3T_2-1712A_{-2}T_0^2T_1T_2^2-90A_{-2}A_0A_1T_0\\
&-90A_{-2}A_{-1}A_2T_0-180A_{-2}A_{-1}A_1T_1-270A_{-2}A_{-1}A_0T_2-30A_{-1}A_1T_0^2T_1\\
&-105A_{-1}A_0T_0T_1^2-120A_{-1}A_0T_0^2T_2-345A_{-1}^2T_0T_1T_2-120A_{-2}A_2T_0^2T_1\\
&-780A_{-2}A_0T_0T_1T_2-31A_{-1}T_0T_1^4-136A_{-1}T_0^3T_2^2-9A_{-1}cT_0-15A_{-1}A_2T_0^3\\
&-18A_{-2}cT_1-45A_{-1}A_0^2T_0-45A_{-1}^2A_1T_0-90A_{-1}^2A_0T_1-90A_{-2}A_0^2T_1\\
&-120A_{-2}A_0T_1^3-90A_{-2}^2A_2T_1-135A_{-2}^2A_1T_2-690A_{-2}^2T_1T_2^2-32A_{-2}T_1^5\\
&-45A_{-1}^3T_2-\tfrac{105}{2}A_{-1}^2T_1^3=0,
\end{aligned}
$$

$$
\begin{aligned}
[E(\theta)]^{-1}:\ & -272A_{-2}T_0^2T_2^3-584A_{-2}T_0T_1^2T_2^2-62A_{-2}T_1^4T_2-136A_{-1}T_0^2T_1T_2^2-52A_{-1}T_0T_1^3T_2\\
&-A_{-1}T_1^5-150A_{-2}^2T_2^3-465A_{-2}A_{-1}T_1T_2^2-240A_{-2}A_0T_0T_2^2-210A_{-2}A_0T_1^2T_2\\
&-210A_{-2}A_1T_0T_1T_2-30A_{-2}A_1T_1^3-60A_{-2}A_2T_0^2T_2-60A_{-2}A_2T_0T_1^2\\
&-105A_{-1}^2T_0T_2^2-90A_{-1}^2T_1^2T_2-120A_{-1}A_0T_0T_1T_2-15A_{-1}A_0T_1^3-15A_{-1}A_1T_0^2T_2\\
&-15A_{-1}A_1T_0T_1^2-15A_{-1}A_2T_0^2T_1-90A_{-2}^2A_2T_2-180A_{-2}A_{-1}A_1T_2\\
&-90A_{-2}A_{-1}A_2T_1-90A_{-2}A_0^2T_2-90A_{-2}A_0A_1T_1-90A_{-1}^2A_0T_2-45A_{-1}^2A_1T_1\\
&-45A_{-1}A_0^2T_1-18A_{-2}cT_2-9A_{-1}cT_1=0,
\end{aligned}
$$

$$
\begin{aligned}
[E(\theta)]^{0}:\ & -22A_{-1}T_0T_1^2T_2^2-120A_{-2}T_0T_1T_2^3+30A_{-1}A_2T_0T_1^2+45A_{-1}A_2T_0^2T_2\\
&-15A_{-1}A_0T_1^2T_2-30A_{-1}A_0T_0T_2^2-30A_{-2}A_1T_1^2T_2-45A_{-2}A_1T_0T_2^2\\
&-90A_{-2}A_0T_1T_2^2+120A_2T_0^3T_1T_2+22A_1T_0^2T_1^2T_2+90A_{-1}A_0A_2T_0\\
&+90A_{-2}A_1A_2T_0-90A_{-2}A_0A_1T_2-90A_{-2}A_{-1}A_2T_2\\
&+90A_0A_2T_0^2T_1+15A_0A_1T_0T_1^2-16A_{-1}T_0^2T_2^3-A_{-1}T_1^4T_2+\tfrac{75}{2}A_1^2T_0^2T_1\\
&+75A_1A_2T_0^3-30A_{-2}T_1^3T_2^2+9cA_1T_0+16A_1T_0^3T_2^2+A_1T_0T_1^4+30A_2T_0^2T_1^3\\
&-75A_{-2}A_{-1}T_2^3-\tfrac{75}{2}A_{-1}^2T_1T_2^2-45A_{-1}A_0^2T_2+45A_{-1}A_1^2T_0+45A_0^2A_1T_0\\
&-45A_{-1}^2A_1T_2-9A_{-1}cT_2+30A_0A_1T_0^2T_2=0,
\end{aligned}
$$

$$
\begin{aligned}
[E(\theta)]^{1}:\ & 136A_1T_0^2T_1T_2^2+52A_1T_0T_1^3T_2+A_1T_1^5+272A_2T_0^3T_2^2+584A_2T_0^2T_1^2T_2+62A_2T_0T_1^4\\
&+15A_{-2}A_1T_1T_2^2+60A_{-2}A_2T_0T_2^2+60A_{-2}A_2T_1^2T_2+15A_{-1}A_1T_0T_2^2\\
&+15A_{-1}A_1T_1^2T_2+210A_{-1}A_2T_0T_1T_2+30A_{-1}A_2T_1^3+120A_0A_1T_0T_1T_2\\
&+15A_0A_1T_1^3+240A_0A_2T_0^2T_2+210A_0A_2T_0T_1^2+105A_1^2T_0^2T_2+90A_1^2T_0T_1^2\\
&+465A_1A_2T_0^2T_1+150A_2^2T_0^3+90A_{-2}A_1A_2T_1+90A_{-2}A_2^2T_0+90A_{-1}A_0A_2T_1\\
&+45A_{-1}A_1^2T_1+180A_{-1}A_1A_2T_0+45A_0^2A_1T_1+90A_0^2A_2T_0+90A_0A_1^2T_0+9cA_1T_1\\
&+18cA_2T_0=0,
\end{aligned}
$$

$$
\begin{aligned}
[E(\theta)]^2 : {}& 45A_1^3T_0 + \frac{105}{2}A_1^2T_1^3 + 32A_2T_1^5 + 195A_{-1}A_2T_0T_2^2 + 180A_{-1}A_2T_1^2T_2 \\
&+ 120A_{-2}A_2T_1T_2^2 + 30A_{-1}A_1T_1T_2^2 + 292A_1T_0T_1^2T_2^2 + 1712A_2T_0^2T_1T_2^2 \\
&+ 884A_2T_0T_1^3T_2 + 270A_0A_1A_2T_0 + 180A_{-1}A_1A_2T_1 + 90A_{-1}A_0A_2T_2 \\
&+ 90A_{-2}A_1A_2T_2 + 795A_1A_2T_0^2T_2 + 750A_1A_2T_0T_1^2 + 105A_0A_1T_1^2T_2 \\
&+ 345A_1^2T_0T_1T_2 + 120A_0A_1T_0T_2^2 + 120A_0A_2T_1^3 + 18cA_2T_1 + 9cA_1T_2 \\
&+ 15A_{-2}A_1T_2^3 + 31A_1T_1^4T_2 + 136A_1T_0^2T_2^3 + 90A_0A_1^2T_1 + 90A_0^2A_2T_1 \\
&+ 45A_0^2A_1T_2 + 135A_{-1}A_2^2T_0 + 45A_{-1}A_1^2T_2 + 90A_{-2}A_2^2T_1 + 690A_2^2T_0^2T_1 \\
&+ 780A_0A_2T_0T_1T_2 = 0,
\end{aligned}
$$

$$
\begin{aligned}
[E(\theta)]^3 : {}& 480A_1T_0T_1T_2^3 + 180A_1T_1^3T_2^2 + 1232A_2T_0^2T_2^3 + 3104A_2T_0T_1^2T_2^2 + 422A_2T_1^4T_2 \\
&+ 60A_{-2}A_2T_2^3 + 15A_{-1}A_1T_2^3 + 285A_{-1}A_2T_1T_2^2 + 180A_0A_1T_1T_2^2 + 600A_0A_2T_0T_2^2 \\
&+ 570A_0A_2T_1^2T_2 + 270A_1^2T_0T_2^2 + 255A_1^2T_1^2T_2 + 2250A_1A_2T_0T_1T_2 + 360A_1A_2T_1^3 \\
&+ 990A_2^2T_0^2T_2 + 960A_2^2T_0T_1^2 + 90A_{-2}A_2^2T_2 + 180A_{-1}A_1A_2T_2 + 135A_{-1}A_2^2T_1 \\
&+ 90A_0^2A_2T_2 + 90A_0A_1^2T_2 + 270A_0A_1A_2T_1 + 180A_0A_2^2T_0 + 45A_1^3T_1 + 180A_1^2A_2T_0 \\
&+ 18cA_2T_2 = 0,
\end{aligned}
$$

$$
\begin{aligned}
[E(\theta)]^4 : {}& 180A_1^2A_2T_1 + 180A_0A_2^2T_1 + 1710A_2T_1^3T_2^2 + 390A_1T_1^2T_2^3 + 240A_1T_0T_2^4 \\
&+ 135A_{-1}A_2^2T_2 + 45A_1^3T_2 + 420A_2^2T_1^3 + \tfrac{735}{2}A_1^2T_1T_2^2 + 90A_0A_1T_2^3 \\
&+ 135A_2A_{-1}T_2^3 + 270A_0A_1A_2T_2 + 2580T_0A_2^2T_1T_2 + 1500A_1A_2T_1^2T_2 \\
&+ 1545T_0A_1A_2T_2^2 + 810A_0A_2T_1T_2^2 + 3960A_2T_0T_1T_2^3 + 225A_1A_2^2T_0 = 0,
\end{aligned}
$$

$$
\begin{aligned}
[E(\theta)]^5 : {}& 360A_1T_1T_2^4 + 1680A_2T_0T_2^4 + 3000A_2T_1^2T_2^3 + 360A_0A_2T_2^3 + 165A_1^2T_2^3 \\
&+ 1965A_1A_2T_1T_2^2 + 1650A_2^2T_0T_2^2 + 1620A_2^2T_1^2T_2 + 180A_0A_2^2T_2 + 180A_1^2A_2T_2 \\
&+ 225A_1A_2^2T_1 + 90A_2^3T_0 = 0,
\end{aligned}
$$

$$
\begin{aligned}
[E(\theta)]^6 : {}& 120A_1T_2^5 + 2400A_2T_1T_2^4 + 825A_1A_2T_2^3 + 2010A_2^2T_1T_2^2 + 225A_1A_2^2T_2 \ + \\
& 90A_2^3T_1 = 0,
\end{aligned}
$$

$$
[E(\theta)]^7 : 720A_2T_2^5 + 810A_2^2T_2^3 + 90A_2^3T_2 = 0.
$$

The above system yields multiple solution sets. The resulting algebraic equations are solved using Wolfram Mathematica (Version 14.2).

$$
\textbf{Set 1:} \begin{Bmatrix} A_{-2} = 0, \quad A_{-1} = 0, \quad A_0 = -\dfrac{2}{3}(8T_0^2 + T_1^2), \\ A_1 = -8T_0T_1, \quad A_2 = -8T_0^2, \quad c = -\dfrac{11}{9}(4T_0^2 - T_1^2)^2. \end{Bmatrix}
$$

$$\textbf{Set 2: } \begin{Bmatrix} A_{-2} = 0, \quad A_{-1} = 0, \quad A_0 = \frac{1}{12}\left(-8T_0^2 - T_1^2\right), \\ A_1 = -T_0T_1, \quad A_2 = -T_0^2, \quad c = -\frac{1}{144}\left(4T_0^2 - T_1^2\right)^2. \end{Bmatrix}$$

$$\textbf{Set 3: } \begin{Bmatrix} A_{-2} = -T_0^2, \quad A_{-1} = -T_0T_1, \quad A_0 = \frac{1}{12}\left(-8T_0^2 - T_1^2\right), \\ A_1 = -T_0T_1, \quad A_2 = -T_0^2, \quad c = \frac{1}{144}\left(-256T_0^4 - 112T_0^2T_1^2 - T_1^4\right). \end{Bmatrix}$$

Using the above solution set along with Eqs (2.8) and (2.2), and Table 1, leads to the following solution function of Eq (1.3).

We discuss only those cases that produce physically meaningful wave structures. Cases 1 and 2 are omitted because they yield only constant solutions and do not provide additional information about the wave behavior of the considered model. Therefore, only Cases 3–9 are presented and analyzed in detail.

Set 1:

Case 3: If $T_0 = \frac{1}{2}$, $T_1 = 0$, $T_2 = -\frac{1}{2}$, and $A_2 \neq 0$, then the solution is

$$u_1(x,t) = -\frac{4}{3} - 2(\tanh(x+ct) + i\operatorname{sech}(x+ct))^2. \tag{2.10}$$

Case 4: If $T_0 = 1$, $T_1 = 0$, $T_2 = -1$, and $A_2 \neq 0$, then the solution is

$$u_2(x,t) = -8\tanh^2(x+ct) - \frac{16}{3}. \tag{2.11}$$

Case 5: After inserting $T_0 = \frac{1}{2}$, $T_1 = 0$, $T_2 = \frac{1}{2}$, and $A_2 \neq 0$, the solution is

$$u_3(x,t) = -2(\tan(x+ct) + \operatorname{sech}(x+ct))^2 - \frac{4}{3}. \tag{2.12}$$

Case 6: By applying $T_0 = -\frac{1}{2}$, $T_1 = 0$, $T_2 = -\frac{1}{2}$, and $A_2 \neq 0$, the solution is

$$u_4(x,t) = -2(\cot(x+ct) + \csc(x+ct))^2 - \frac{4}{3}. \tag{2.13}$$

Case 7: Substituting of $T_0 = 1$, $T_1 = 0$, $T_2 = 1$, and $A_2 \neq 0$, the solution is

$$u_5(x,t) = -8\tan^2(x+ct) - \frac{16}{3}. \tag{2.14}$$

Case 8: Substituting $T_0 = -1$, $T_1 = 0$, $T_2 = -1$, and $A_2 \neq 0$, the solution is

$$u_6(x,t) = -8\cot^2(x+ct) - \frac{16}{3}. \tag{2.15}$$

Case 9: With $T_0 = Constant$, $A_2 \neq 0$, $T_2 = 0$, and $T_1 \neq 0$, the resulting solution is given by

$$u_7(x,t) = -\frac{8\left(e^{x+ctS} - R\right)^2}{S^2} - \frac{8\left(e^{x+ctS} - R\right)}{S} - 6. \tag{2.16}$$

Set 2:

Case 3: If $T_0 = \frac{1}{2}$, $T_1 = 0$, $T_2 = -\frac{1}{2}$, and $A_2 \neq 0$, then the solution is

$$u_8(x,t) = -\frac{1}{6} - \frac{1}{4}(\tanh(x+ct) + i\operatorname{sech}(x+ct))^2. \tag{2.17}$$

Case 4: If $T_0 = 1$, $T_1 = 0$, $T_2 = -1$, and $A_2 \neq 0$, then the solution is

$$u_9(x,t) = -\tanh^2(x+ct) - \frac{2}{3}. \tag{2.18}$$

Case 5: After inserting $T_0 = \frac{1}{2}$, $T_1 = 0$, $T_2 = \frac{1}{2}$, and $A_2 \neq 0$, the solution is

$$u_{10}(x,t) = -\frac{1}{4}(\tan(x+ct) + \operatorname{sech}(x+ct))^2 - \frac{1}{6}. \tag{2.19}$$

Case 6: By applying $T_0 = -\frac{1}{2}$, $T_1 = 0$, $T_2 = -\frac{1}{2}$, and $A_2 \neq 0$, the solution is

$$u_{11}(x,t) = -\frac{1}{4}(\cot(x+ct) + \csc(x+ct))^2 - \frac{1}{6}. \tag{2.20}$$

Case 7: Substituting $T_0 = 1$, $T_1 = 0$, $T_2 = 1$, and $A_2 \neq 0$, the solution is

$$u_{12}(x,t) = -\tan^2(x+ct) - \frac{2}{3}. \tag{2.21}$$

Case 8: Substituting $T_0 = -1$, $T_1 = 0$, $T_2 = -1$, and $A_2 \neq 0$, the solution is

$$u_{13}(x,t) = -\cot^2(x+ct) - \frac{2}{3}. \tag{2.22}$$

Case 9: With $T_0 = Constant$, $A_2 \neq 0$, $T_2 = 0$, and $T_1 \neq 0$, the resulting solution is given by

$$u_{14}(x,t) = -\frac{\left(e^{x+ctS} - R\right)^2}{S^2} - \frac{e^{x+ctS} - R}{S} - \frac{3}{4}. \tag{2.23}$$

Set 3:

Case 3: If $T_0 = \frac{1}{2}$, $T_1 = 0$, $T_2 = -\frac{1}{2}$, and $A_2 \neq 0$, then the solution is

$$u_{15}(x,t) = -\frac{1}{4}(\tanh(x+ct) + i\operatorname{sech}(x+ct))^2 - \frac{1}{4(\tanh(x+ct) + i\operatorname{sech}(x+ct))^2} - \frac{1}{6}. \tag{2.24}$$

Case 4: If $T_0 = 1$, $T_1 = 0$, $T_2 = -1$, and $A_2 \neq 0$, then the solution is

$$u_{16}(x,t) = -\tanh^2(x+ct) - \coth^2(x+ct) - \frac{2}{3}. \tag{2.25}$$

Case 5: After inserting $T_0 = \frac{1}{2}$, $T_1 = 0$, $T_2 = \frac{1}{2}$, and $A_2 \neq 0$, the solution is

$$u_{17}(x,t) = -\frac{1}{4}(\tan(x+ct) + \operatorname{sech}(x+ct))^2 - \frac{1}{4(\tan(x+ct) + \operatorname{sech}(x+ct))^2} - \frac{1}{6}. \tag{2.26}$$

Case 6: By applying $T_0 = -\frac{1}{2}$, $T_1 = 0$, $T_2 = -\frac{1}{2}$, and $A_2 \neq 0$, the solution is

$$u_{18}(x,t) = -\frac{1}{4}(\cot(x+ct) + \csc(x+ct))^2 - \frac{1}{4(\cot(x+ct) + \csc(x+ct))^2} - \frac{1}{6}. \tag{2.27}$$

Case 7: Substituting $T_0 = 1$, $T_1 = 0$, $T_2 = 1$, and $A_2 \neq 0$, the solution is

$$u_{19}(x,t) = -\tan^2(x+ct) - \cot^2(x+ct) - \frac{2}{3}. \tag{2.28}$$

Case 8: Substituting $T_0 = -1$, $T_1 = 0$, $T_2 = -1$, and $A_2 \neq 0$, the solution is

$$u_{20}(x,t) = -\tan^2(x+ct) - \cot^2(x+ct) - \frac{2}{3}. \tag{2.29}$$

Case 9: With $T_0 = Constant$, $A_2 \neq 0$, $T_2 = 0$, and $T_1 \neq 0$, the resulting solution is given by

$$u_{21}(x,t) = -\frac{\left(e^{x+ctS} - R\right)^2}{S^2} - \frac{S^2}{(e^{x+ctS} - R)^2} - \frac{e^{x+ctS} - R}{S} - \frac{S}{e^{x+ctS} - R} - \frac{3}{4}. \tag{2.30}$$

3. The $G'/(bG' + G + a)$-expansion technique

Assume that the solution of the reduced ODE can be written as:

$$U(\theta) = \sum_{i=0}^{N} A_i F^i(\theta), \tag{3.1}$$

where the coefficients A_i ($i = 0, 1, 2, \ldots, N$) represent unknown parameters to be evaluated, while the positive integer N is determined by applying the homogeneous balance principle. Here,

$$F = F(\theta) = \frac{G'}{bG' + G + a},$$

a and b are non-zero parameters ($b \neq 0$), and $G = G(\theta)$ satisfies the following auxiliary differential equation:

$$G'' = -\frac{\lambda}{b}G' - \frac{\lambda}{b^2}G - \frac{\mu a}{b^2}, \tag{3.2}$$

where λ and μ are real constants.

Differentiating $F(\theta) = \frac{G'}{bG'+G+a}$ with respect to θ and applying the quotient rule produces an expression involving G, G', and G''. By substituting the auxiliary differential equation given in Eq (3.2) into the resulting expression and simplifying the obtained terms, the Riccati-type equation is obtained:

$$F' = -\frac{\mu}{b^2} + \frac{(2\mu - \lambda)}{b}F + (\lambda - \mu - 1)F^2. \tag{3.3}$$

To avoid singularities or undefined expressions, the restrictions $b \neq 0$ with $\lambda - \mu - 1 \neq 0$ have been imposed where required in the analysis. Moreover, the admissible parameteric domains in correspondence with hyperbolic, trigonometric, or rational solution are extracted according to discriminant restrictions arising from Eq (3.3).

Type 1: If $\Lambda = \lambda^2 - 4\mu > 0$, then $G = -a + p_1 e^{\frac{1}{2b}(-\lambda-\sqrt{\Lambda})\theta} + p_2 e^{\frac{1}{2b}(-\lambda+\sqrt{\Lambda})\theta}$, p_1, and p_2 are arbitrary constants satisfying $a^2 + p_1^2 + p_2^2 \neq 0$.

In this case, $F = F(\theta)$ can be represented as follows:

$$F = \frac{p_1(\lambda + \sqrt{\Lambda}) + p_2(\lambda - \sqrt{\Lambda})e^{\frac{\sqrt{\Lambda}}{b}\theta}}{b\, p_1(\lambda - 2 + \sqrt{\Lambda}) + b\, p_2(\lambda - 2 - \sqrt{\Lambda})e^{\frac{\sqrt{\Lambda}}{b}\theta}}. \tag{3.4}$$

The function $F = F(\theta)$ admits the following equivalent hyperbolic representation:

$$F = \frac{\Big(\lambda(p_2 - p_1) - \sqrt{\Lambda}(p_2 + p_1)\Big)\sinh(\frac{\sqrt{\Lambda}}{2b}\theta) + \Big(\lambda(p_2 + p_1) - \sqrt{\Lambda}(p_2 - p_1)\Big)\cosh(\frac{\sqrt{\Lambda}}{2b}\theta)}{b\Big((\lambda - 2)(p_2 - p_1) - \sqrt{\Lambda}(p_2 + p_1)\Big)\sinh(\frac{\sqrt{\Lambda}}{2b}\theta) + b\Big((\lambda - 2)(p_2 + p_1) - \sqrt{\Lambda}(p_2 - p_1)\Big)\cosh(\frac{\sqrt{\Lambda}}{2b}\theta)}.$$

- If $(\lambda - 2)(p_2 - p_1) - \sqrt{\Lambda}(p_2 + p_1) = 0$, then

$$F = \frac{\lambda - 2\mu}{2b(\lambda - \mu - 1)} - \frac{\sqrt{\Lambda}}{2b(\lambda - \mu - 1)}\tanh(\frac{\sqrt{\Lambda}}{2b}\theta). \tag{3.5}$$

- If $(\lambda - 2)(p_2 + p_1) - \sqrt{\Lambda}(p_2 - p_1) = 0$, then

$$F = \frac{\lambda - 2\mu}{2b(\lambda - \mu - 1)} - \frac{\sqrt{\Lambda}}{2b(\lambda - \mu - 1)}\coth(\frac{\sqrt{\Lambda}}{2b}\theta). \tag{3.6}$$

Type 2: If $\Lambda = \lambda^2 - 4\mu < 0$, then $G = -a + e^{\frac{-\lambda}{2b}\theta}\Big(p_1\cos(\frac{\sqrt{-\Lambda}}{2b}\theta) + p_2\sin(\frac{\sqrt{-\Lambda}}{2b}\theta)\Big)$.

In this case of type 2, the function $F = F(\theta)$ can be written in the following representation:

$$F = \frac{\Big(\lambda p_1 - \sqrt{-\Lambda}p_2\Big)\cos(\frac{\sqrt{-\Lambda}}{2b}\theta) + \Big(\lambda p_2 - \sqrt{-\Lambda}p_1\Big)\sin(\frac{\sqrt{-\Lambda}}{2b}\theta)}{b\Big((\lambda - 2)p_1 - \sqrt{-\Lambda}p_2\Big)\cos(\frac{\sqrt{-\Lambda}}{2b}\theta) + b\Big((\lambda - 2)p_2 + \sqrt{-\Lambda}p_1\Big)\sin(\frac{\sqrt{-\Lambda}}{2b}\theta)}. \tag{3.7}$$

- If $(\lambda - 2)p_2 + \sqrt{-\Lambda}p_1 = 0$, then

$$F = \frac{\lambda - 2\mu}{2b(\lambda - \mu - 1)} + \frac{\sqrt{-\Lambda}}{2b(\lambda - \mu - 1)}\tan(\frac{\sqrt{-\Lambda}}{2b}\theta). \tag{3.8}$$

- If $(\lambda - 2)p_1 - \sqrt{-\Lambda}p_2 = 0$, then

$$F = \frac{\lambda - 2\mu}{2b(\lambda - \mu - 1)} - \frac{\sqrt{-\Lambda}}{2b(\lambda - \mu - 1)}\cot(\frac{\sqrt{-\Lambda}}{2b}\theta). \tag{3.9}$$

By substituting Eqs (3.1) and (3.3) in the transformed ODE, followed by setting the coefficients of F^i equal to zero, we produce a system of algebraic equations. Solving this system yields the values of the arbitrary constants.

3.1. Application of the $G'/(bG'+G+a)$-expansion method

Consider the solution of (2.7) as:

$$U = A_0 + A_1 F + A_2 F^2. \tag{3.10}$$

By substituting Eq (3.10) into Eq (2.7) and equating the coefficients of the terms F^0, F, F^2, F^3, F^4, F^5, F^6, and F^7 to zero yields a system of algebraic equations. Solving this system yields the following set of solutions:

$$\left\{A_0 = -\tfrac{2\left(\lambda^2-12\lambda\mu+4\mu(3\mu+2)\right)}{3b^2}, A_1 = \tfrac{8(\lambda-2\mu)(\lambda-\mu-1)}{b}, A_2 = -8(-\lambda+\mu+1)^2, c = -\tfrac{11\left(\lambda^2-4\mu\right)^2}{9b^4}\right\}.$$

Type 1: If $\Lambda = \lambda^2 - 4\mu > 0$, then we obtain:

$$u(x,t) = -\frac{8}{b^2}\Big[(\lambda-2\mu)(\lambda-\mu-1)F + (\mu+1-\lambda)^2F^2\Big] + \frac{2\left(-\lambda^2+12\lambda\mu-12\mu^2-8\mu\right)}{3b^2}, \tag{3.11}$$

where

$$F = \frac{p_2\left(\lambda-\sqrt{\Lambda}\right)e^{\frac{\sqrt{\Lambda}x}{b}} + p_1\left(\lambda+\sqrt{\Lambda}\right)}{p_2\left(-\lambda+\sqrt{\Lambda}+2\right)e^{\frac{\sqrt{\Lambda}x}{b}} - p_1\left(\lambda+\sqrt{\Lambda}-2\right)}.$$

- If $(\lambda-2)(p_2-p_1) - \sqrt{\Lambda}(p_2+p_1) = 0$, then

$$u(x,t) = \frac{2\left(-3\Lambda\tanh^2\left(\frac{\theta\sqrt{\Lambda}}{2b}\right) + 2\lambda^2 - 8\mu\right)}{3b^2}. \tag{3.12}$$

- If $(\lambda-2)(p_2+p_1) - \sqrt{\Lambda}(p_2-p_1) = 0$, then

$$u(x,t) = \frac{2\left(-3\Lambda\coth^2\left(\frac{\theta\sqrt{\Lambda}}{2b}\right) + 2\lambda^2 - 8\mu\right)}{3b^2}. \tag{3.13}$$

Type 2: If $\Lambda = \lambda^2 - 4\mu < 0$, then we obtain:

$$\begin{aligned} u(x,t) = &-\frac{2\left(\lambda^2-12\lambda\mu+4\mu(3\mu+2)\right)}{3b^2} \\ &- \frac{8(-\lambda+\mu+1)^2\Big[\cos\!\Big(\frac{\theta\sqrt{-\Lambda}}{2b}\Big)(\lambda p_1 - \sqrt{-\Lambda}\,p_2) + \sin\!\Big(\frac{\theta\sqrt{-\Lambda}}{2b}\Big)(\lambda p_2 - \sqrt{-\Lambda}\,p_2)\Big]^2}{\Big[b\cos\!\Big(\frac{\theta\sqrt{-\Lambda}}{2b}\Big)((\lambda-2)p_1 - \sqrt{-\Lambda}\,p_2) + b\sin\!\Big(\frac{\theta\sqrt{-\Lambda}}{2b}\Big)((\lambda-2)p_2 - \sqrt{-\Lambda}\,p_2)\Big]^2} \\ &+ \frac{8(\lambda-\mu-1)(\lambda-2\mu)\Big[\cos\!\Big(\frac{\theta\sqrt{-\Lambda}}{2b}\Big)(\lambda p_1 - \sqrt{-\Lambda}\,p_2) + \sin\!\Big(\frac{\theta\sqrt{-\Lambda}}{2b}\Big)(\lambda p_2 - \sqrt{-\Lambda}\,p_2)\Big]}{b\Big[b\cos\!\Big(\frac{\theta\sqrt{-\Lambda}}{2b}\Big)((\lambda-2)p_1 - \sqrt{-\Lambda}\,p_2) + b\sin\!\Big(\frac{\theta\sqrt{-\Lambda}}{2b}\Big)((\lambda-2)p_2 - \sqrt{-\Lambda}\,p_2)\Big]}. \end{aligned} \tag{3.14}$$

- If $(\lambda-2)p_2 + \sqrt{-\Lambda}p_1 = 0$, then

$$u(x,t) = \frac{2\left(-3\Lambda\tanh^2\left(\frac{\theta\sqrt{\Lambda}}{2b}\right) + 2\lambda^2 - 8\mu\right)}{3b^2}. \tag{3.15}$$

- If $(\lambda - 2)p_1 - \sqrt{-\Lambda}p_2 = 0$, then

$$u(x,t) = \frac{2\left(-3\Lambda\coth^2\left(\frac{\theta\sqrt{\Lambda}}{2b}\right) + 2\lambda^2 - 8\mu\right)}{3b^2}. \tag{3.16}$$

For the validation of the obtained solutions, each analytical solution was substituted into the corresponding reduced ODE. The required derivatives were evaluated symbolically with the help of Mathematica, and after simplification, the resulting expressions became identically zero. Hence, the obtained analytical solutions satisfy the governing equation under the stated parameter conditions.

4. Graphical representation

In this section, the dynamical characteristics of the derived solutions are analyzed through graphical visualization. To improve the presentation of the obtained results, only non-repeated and physically significant solutions are included in this study. The obtained wave structures are classified according to their graphical and physical characteristics, including W-shaped soliton, dark, singular, bright, and periodic-singular solutions. The corresponding parameter values are explicitly provided in the captions of each figure. Dark-soliton profiles are characterized by localized intensity depressions that propagate on a continuous, nonzero background, whereas the bright-soliton structures represent stable localized wave pulses. The W-shaped solutions suggest double-localized waveforms exhibiting symmetric propagation. Moreover, the singular and periodic-singular solutions clearly demonstrate localized divergence and oscillatory propagation behavior caused by nonlinear and dispersive effects. Although some obtained solutions contain negative constant shifts, the basic propagation properties of the waves and their stability remain intact during propagation. With the help of Mathematica, various traveling wave solutions, such as rational, trigonometric, and hyperbolic ones, were constructed. 3D, 2D, and contour plots were used to analyze the solitary wave dynamics of the obtained solutions.

For the MFEM, we use different values of c to construct the graph based on the values of T_0, T_1, and T_2, which are mentioned in the Table 1.

Figure 1 shows the dark soliton solution corresponding to Eq (2.10) with parameter value $c = -\frac{11}{9}$. The behavior shows a localized dip in wave amplitude propagating with a continuous non-zero background, which is the characteristic feature of dark-soliton solutions. The wave maintains a stable shape with velocity during propagation. Figures 2–4 show a singular solution to Eqs (2.11)–(2.13) with parameter values $c = -\frac{176}{9}$ and $-\frac{11}{9}$, while Figure 5 shows a singular periodic solution corresponding to Eq (2.14) with parameter value $c = -\frac{176}{9}$.

These profiles exhibit sharp localized singularities, demonstrating the strong nonlinear behavior of the obtained solutions. Figure 6 is the graphical representation of the Eq (2.17), which shows a dark soliton solution with parameter value $c = -\frac{1}{144}$. On the contrary, Figure 7 illustrates a bright profile for Eq (2.18), using parametric value $c = -\frac{1}{9}$, and the solution forms stable localized pulse along concentrated wave energy. Figures 8 and 9 represent periodic singular soliton structures associated with Eqs (2.19) and (2.21), for parameter values $c = -\frac{1}{144}$ and $c = -\frac{1}{9}$, respectively, and exhibit oscillatory wave propagation combined with singular behavior. Figure 10 shows a w-shaped soliton correspond to Eq (2.24) with parameter value $c = -\frac{1}{9}$.

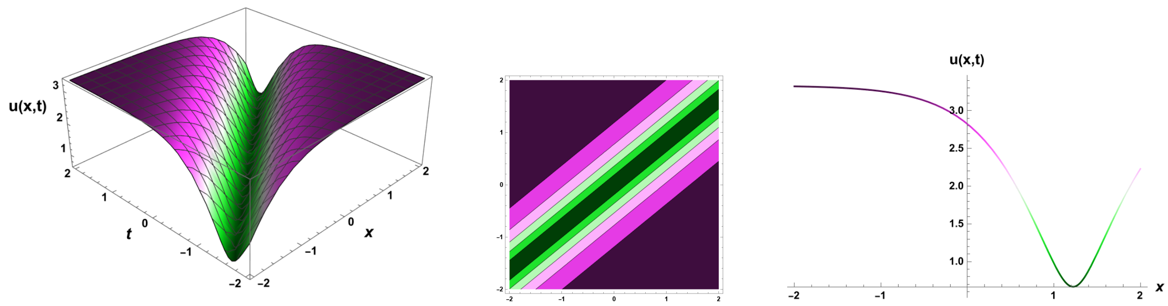

(a) 3D **(b)** Contour **(c)** 2D

Figure 1. 3D, contour, and 2D plots for Eq (2.10) with $c = -\frac{11}{9}$ showing a dark soliton.

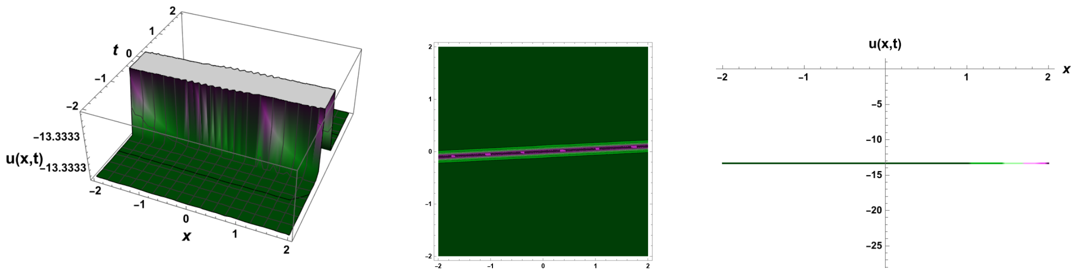

(a) 3D **(b)** Contour **(c)** 2D

Figure 2. A singular solution in 3D, contour and 2D plots for Eq (2.11) with $c = -\frac{176}{9}$ showing a singular soliton solution.

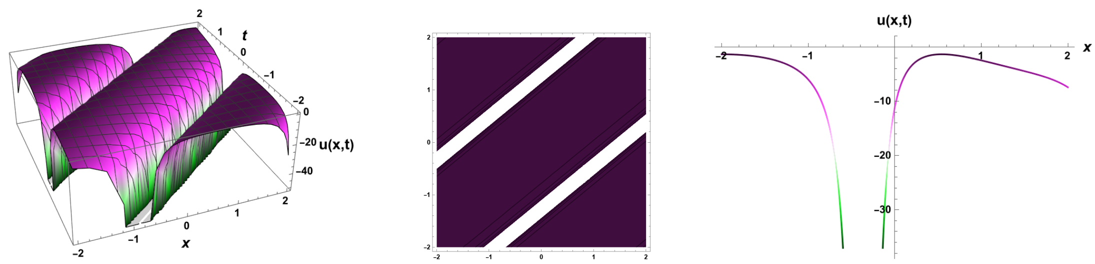

(a) 3D **(b)** Contour **(c)** 2D

Figure 3. 3D, contour, and 2D plots for Eq (2.12) with $c = -\frac{11}{9}$, showing a singluar behavior.

For the $\frac{G'}{bG'+G+a}$-expansion method, Figure 11 gives the graphical illustrations of Eq (3.11), which makes a bright soliton using parametric values $b = 2$, $p_1 = 2$, $\mu = 1$, $p_2 = -1$, and $\lambda = 3$. This wave profile shows a localized bell shape that preserves amplitude during motion, showing the stability of the extracted results. Figure 12 represents the periodic soliton solution for Eq (3.14) for $\lambda = 1$, $\mu = 1$, $p_1 = -2$, $p_2 = 1$, and $b = 2$, where the solution demonstrates repeating wave patterns because of the combined influence of the nonlinearity with dispersion. Overall, the graphical analysis confirms that the considered KK model supports a variety of nonlinear wave structures depending on the selected parameter values. The obtained results verify the effectiveness of the applied analytical methods in describing different propagation behaviors of nonlinear waves.

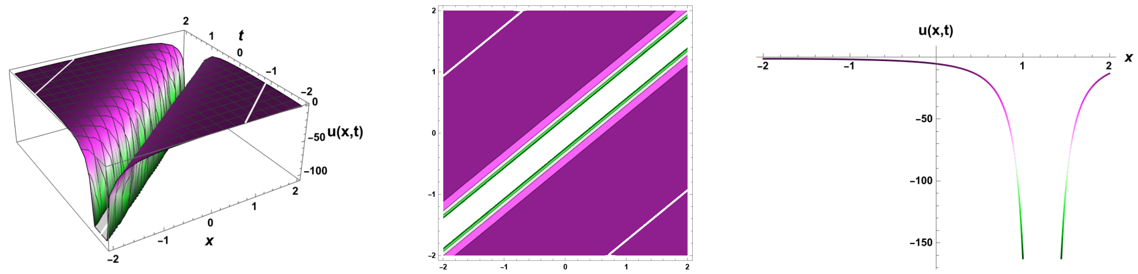

(a) 3D **(b)** Contour **(c)** 2D

Figure 4. A singular solution in 3D, contour, and 2D plots for Eq (2.13) with $c = -\frac{11}{9}$.

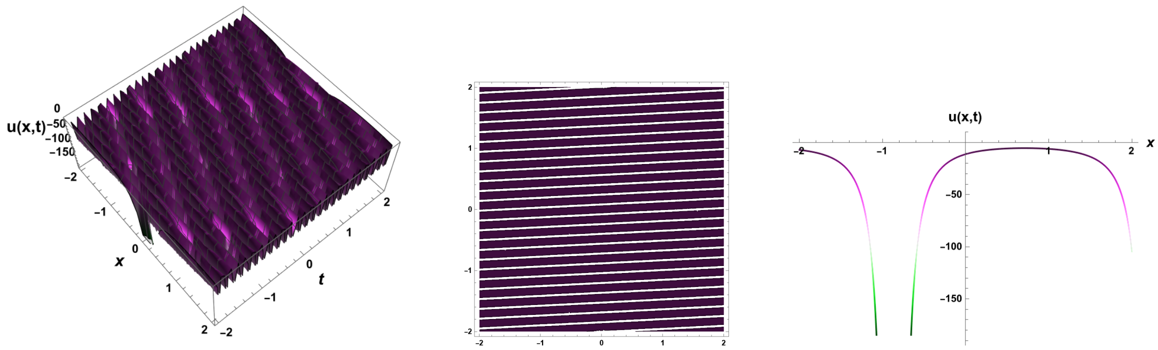

(a) 3D **(b)** Contour **(c)** 2D

Figure 5. A singular periodic solution has been depicted in 3D, contour, and 2D plots for Eq (2.14) with $c = -\frac{176}{9}$.

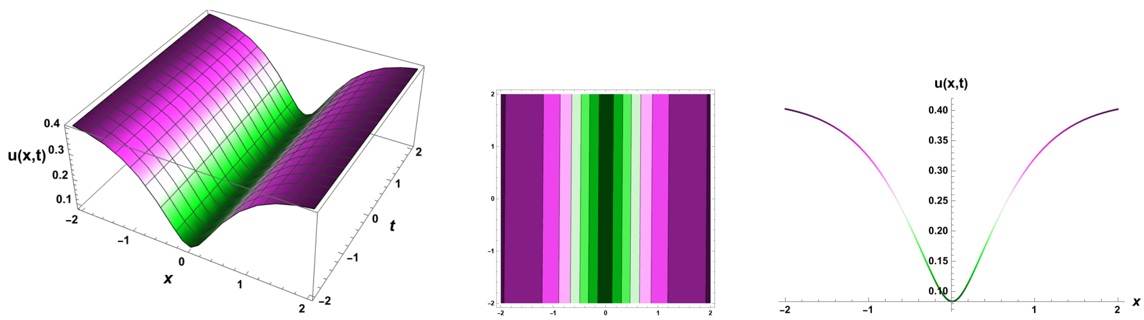

(a) 3D **(b)** Contour **(c)** 2D

Figure 6. A dark soliton in 3D, contour, and 2D plots for Eq (2.17) with $c = -\frac{1}{144}$.

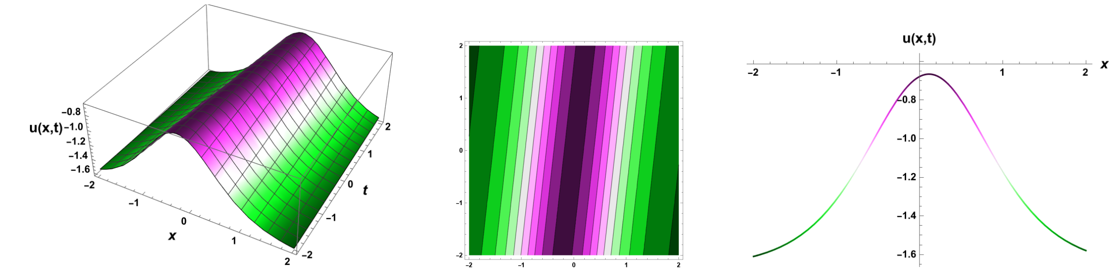

(a) 3D **(b)** Contour **(c)** 2D

Figure 7. A bright soliton as 3D, contour, and 2D plots for Eq (2.18) with $c = -\frac{1}{9}$.

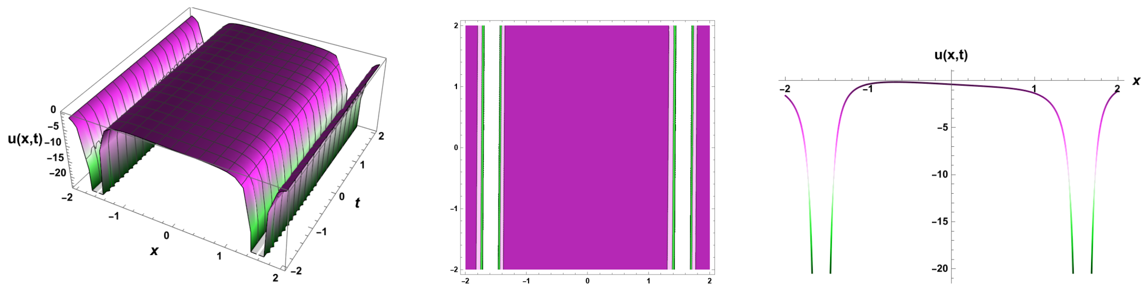

(a) 3D **(b)** Contour **(c)** 2D

Figure 8. A singluar solution as 3D, Contour, and 2D plots for Eq (2.19) with $c = -\frac{1}{144}$.

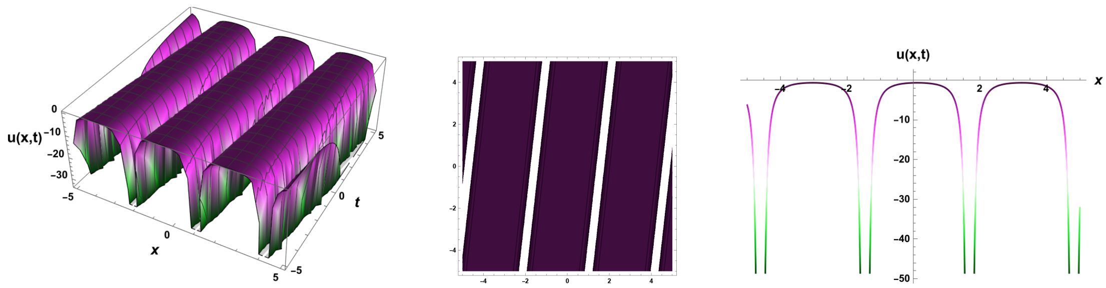

(a) 3D **(b)** Contour **(c)** 2D

Figure 9. 3D, Contour, and 2D plots for Eq (2.21) with $c = -\frac{1}{9}$ showing periodic-singular behavior.

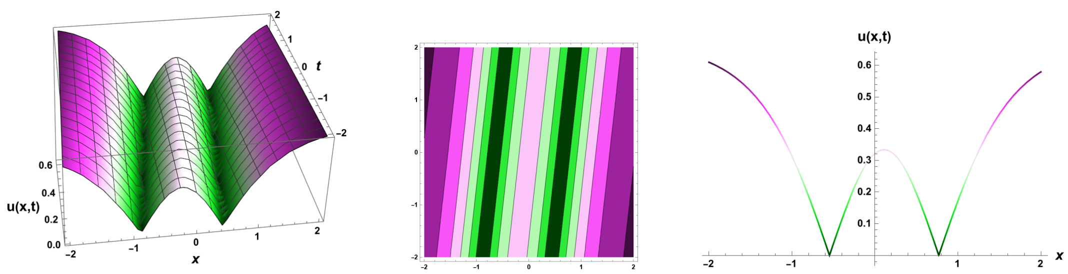

(a) 3D **(b)** Contour **(c)** 2D

Figure 10. A W-shaped soliton as 3D, contour, and 2D plots for Eq (2.24) with $c = -\frac{1}{9}$.

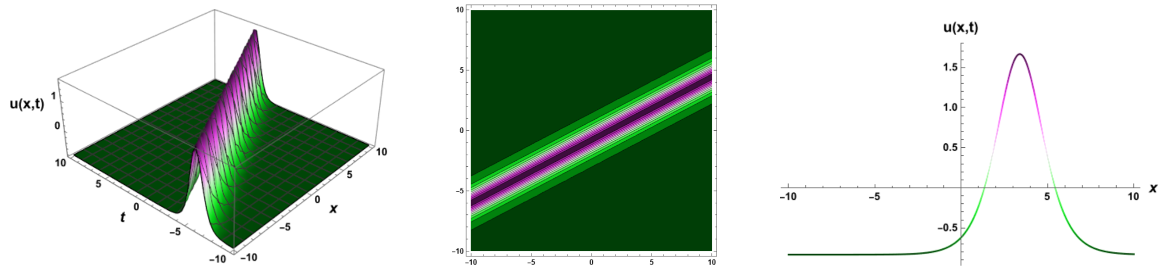

(a) 3D **(b)** Contour **(c)** 2D

Figure 11. A bright soliton as 3D, contour, and 2D plots for Eq (3.11) with $\lambda = 3$, $\mu = 1$, $p_1 = 2$, $p_2 = -1$, and $b = 2$.

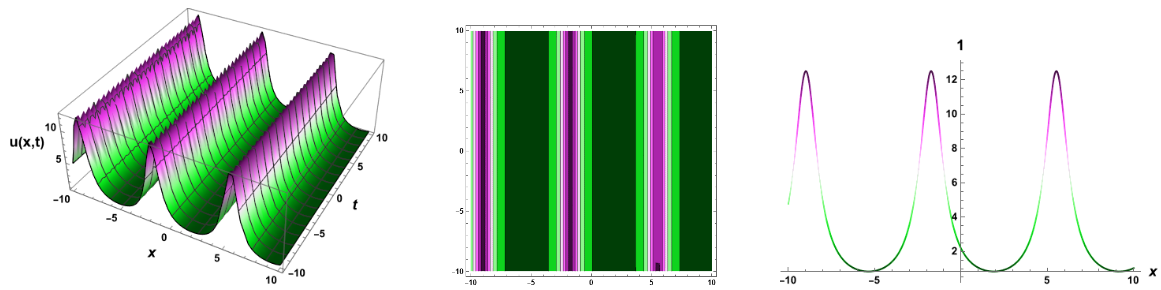

(a) 3D **(b)** Contour **(c)** 2D

Figure 12. Graphical illustration of the periodic soliton solution of Eq (3.14) with $\lambda = 1$, $\mu = 1$, $p_1 = 2$, $p_2 = -1$, and $b = 2$.

5. Modulation instability

Dispersive and nonlinear effects result in the phenomenon of modulation instability (MI). This is a major problem in fiber optic communication systems. In the process of modulation instability, a small disturbance in the signal grows exponentially due to the fundamental nonlinear effect. In the following analysis, we explore modulation instability in Eq (1.3) using the linear stability analysis. Consider the solution to Eq (1.3) given below.

$$u(x,t) = n, \tag{5.1}$$

where n is a real parameter. We have perturbed the steady-state solution by introducing a very tiny disturbance $U(x,t)$:

$$u(x,t) = n + U(x,t), \qquad |U(x,t)| \ll 1. \tag{5.2}$$

Then Eq (1.3) becomes

$$\begin{aligned}45n^2U_x(x,t) + 90nU(x,t)U_x(x,t) + 15nU_{xxx}(x,t) + 9U_t(x,t) + 45U(x,t)^2U_x(x,t)\\ + \frac{75}{2}U_x(x,t)U_{xx}(x,t) + 15U(x,t)U_{xxx}(x,t) + U_{xxxxx}(x,t) = 0.\end{aligned} \tag{5.3}$$

We neglect the higher-order nonlinear perturbation terms

$$UU_x, \qquad U^2U_x, \qquad U_xU_{xx}, \qquad UU_{xxx}.$$

After linearizing the above equation, we get

$$45n^2U_x(x,t) + 15nU_{xxx}(x,t) + 9U_t(x,t) + U_{xxxxx}(x,t) = 0. \tag{5.4}$$

In order to examine the stability of the solution, we use the normal mode perturbation as follows:

$$Q(x,t) = P_1e^{-i(ax-ct)} + Q_1e^{i(ax-ct)}. \tag{5.5}$$

Here, P denotes a small-amplitude constant, ω represents the associated frequency, and $a \in \mathbb{R}$ denotes the wave number of perturbation.

Substituting the above perturbation ansatz into Eq (5.4), we obtain

$$\begin{aligned}&(-i)a^5P_1e^{-i(ax-ct)} + ia^5Q_1e^{i(ax-ct)} + 15ia^3nP_1e^{-i(ax-ct)} - 15ia^3nQ_1e^{i(ax-ct)}\\ -\ & 45ian^2P_1e^{-i(ax-ct)} + 45ian^2Q_1e^{i(ax-ct)} + 9icP_1e^{-i(ax-ct)} - 9icQ_1e^{i(ax-ct)} = 0.\end{aligned} \tag{5.6}$$

After some simplification, we get the following results:

$$c \to \frac{1}{9}\left(a^5 - 15a^3n + 45an^2\right).$$

The dispersion relation is

$$c = \frac{1}{9}\left(a^5 - 15a^3n + 45an^2\right). \tag{5.7}$$

As perturbation wave number a and background amplitude n are real quantities, the frequency ω stays absolutely real. Hence, perturbation evolves within an oscillatory manner without exponential temporal rise. Subsequently, the presented linearized analysis does not show modulation instability in the classical sense. Despite this, the manuscript indicates that a constant background solution is linearly dispersively stable under small perturbations.

A real modulation instability would require ω to have a nonzero imaginary part a, which would rely on the exponential growth of the amplitude. Nothing of this sort of instability region occurs using this dispersion relation.

The dispersion relation (5.4) demonstrates the stability behavior of the steady state. In the case of a real-valued wave number, the steady state is stable when subjected to perturbation. On the other hand, the presence of an imaginary wave number means that the steady state is unstable.

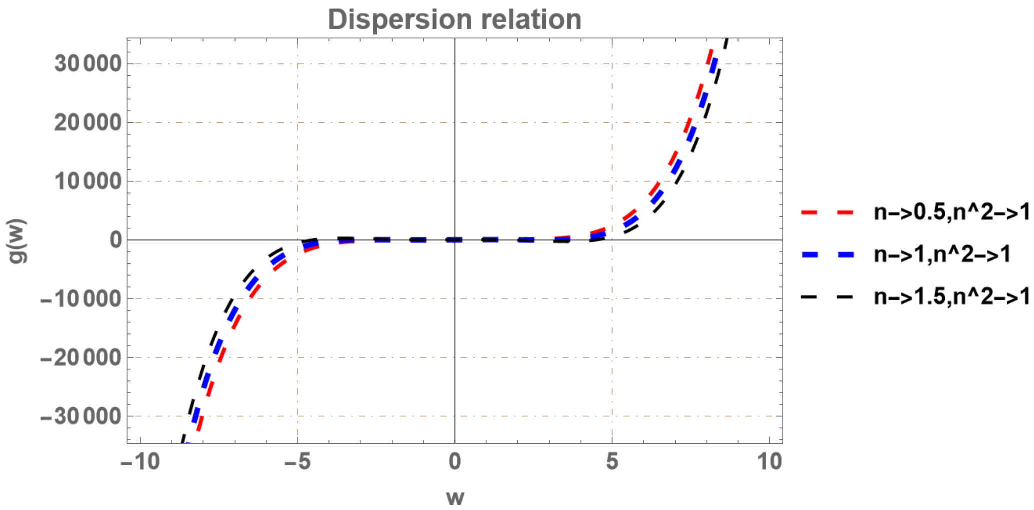

Figure 13. Dispersion relation for increasing n.

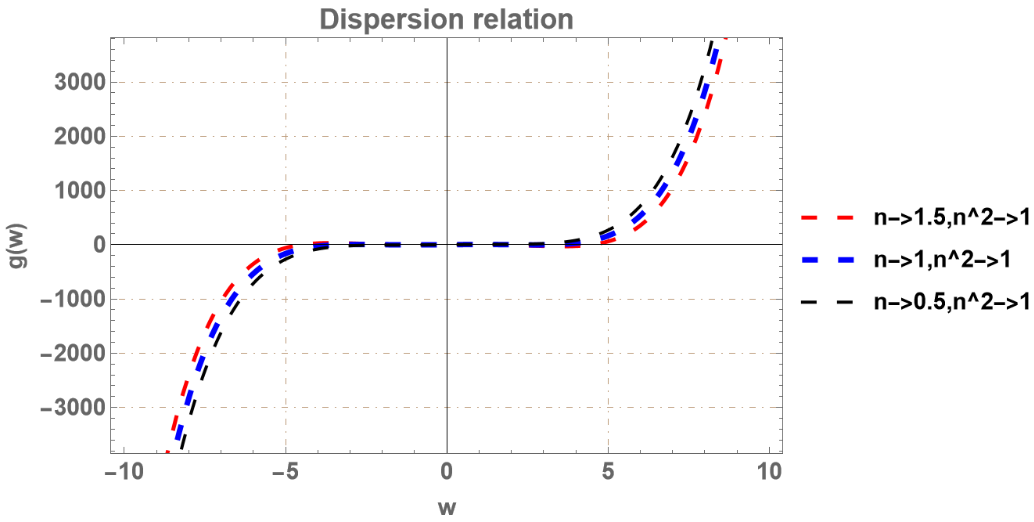

Figure 14. Dispersion relation for decreasing n.

Figures 13 and 14 illustrate variations in the dispersion relation with frequency as n increases or decreases. The curves become more sudden, so stronger dispersion is occurring at higher frequencies for decreasing values of n. The increase in n flattens the curve, showing a weaker dispersion effect.

6. Novelty of the results

The KK equation is a nonlinear equation with a strong nonlinear effect and wave dispersion in (1+1) dimensions. It is a fifth-order equation with a complex form. Although it is a higher-dimensional equation, it preserves a bi-Hamiltonian structure, a Lax pair, and an infinite number of conservation laws. Compared with lower-dimensional equations such as the Korteweg-de Vries (KdV) equation, which mainly describes low-dimensional waves with lower nonlinear effects, the model describes higher-dimensional waves with various kinds of exact solutions, including multi-soliton solutions, rational solutions, periodic solutions, etc. Various methods apply to this equation, but here we discuss this equation with two methods, the $\frac{G'}{bG'+G+a}$-expansion methodology and the MFEM, because these methods are flexible, straightforward, and applicable to a wider range of nonlinear equations. Bright, dark, singular, periodic, and W-shaped solitons are obtained by applying these methods to the proposed model. The solutions obtained include many known results as special cases, which reveal new wave forms with special ways of traveling in the sideways direction. Hence, these results greatly enhance the solutions, which were previously available for the equation, and confirm the effectiveness, reliability, and applicability of the proposed methods for solving complex nonlinear equations in high dimensions. The extracted profiles are consistent with the previously reported wave structures in related literature, including periodic, bright, dark, and singular solitons derived through approaches like the Hirota bilinear method, the (G'/G)-expansion method or tanh function technique. This presented study not only provides several dynamical behaviors of the model but also provides generalized wave structures using the modified F-expansion and $\frac{G'}{bG'+G+a}$-expansion methods. Also, the analysis justifies that the extracted solutions preserve the propagation features with stability properties reported in earlier studies, validating the seemliness with physical applicability of the proposed techniques.

Unlike optimization-based methodologies such as physics informed neural networks, the suggested analytical techniques do not rely on random initials, hyperparameter tuning, and training iterations. So, the issues like variance among repeated runs, convergence instability, and computational sensitivity have been avoided in this study. The modified F-expansion and the $\frac{G'}{bG'+G+a}$-expansion techniques give deterministic structures which yield analytical wave solutions with stable propagation features. Additionally, the obtained solutions are expressed in closed form, which confirms a clearer explanation for nonlinear wave interactions with dispersive dynamics as compared with purely numerical approximations. The study's novelty also lies in the derivation of many new parametric wave families and generalized solution structures, which extend previous results for the governing equation. The findings demonstrate that the proposed techniques are not just computationally appropriate from an analytical point of view but mathematically necessary for investigating higher-order nonlinear evolution models arising in mathematical physics.

Table 2. Comparison of analytical methods applied to the (1+1)-dimensional KK equation.

Method	Solution type	Advantages	Limitations
Fan sub-equation (2011) [46]	Solitary, periodic, elliptic waves	Rich explicit solutions	Mainly traveling waves
(G'/G)-expansion (2013) [47]	Unified traveling waves	Compact representation	Requires Riccati equation
$\exp(-\Phi)$-expansion (2015) [34]	Hyperbolic, trigonometric, rational	Simple algorithm	Limited to polynomial nonlinearities
Double $(G'/G, 1/G)$ (2020) [27]	Bell, kink, periodic waves	Generalized (G'/G) method	Algebraically complex
Modified F-expansion (This work)	Soliton, periodic, hyperbolic waves	Efficient and systematic	Balancing required
$\frac{G'}{bG'+G+a}$**-expansion (This work)**	Generalized soliton and periodic waves	Rich parametric solutions	Algebraically complex

7. Conclusions

In this study, we found the exact analytical solutions to the (1+1)-dimensional KK equation, which is a higher-order nonlinear evolution that arises quite often in mathematical physics. Employing the $\frac{G'}{bG'+G+a}$-expansion technique and the MFEM, various new exact solutions of hyperbolic, trigonometric, and rational types were obtained. Results were shown graphically to highlight the physical characteristics of the solutions. Further, the modulation instability of the equation was discussed to check the behavior of the system when a small disturbance was introduced in the given model. Comparative analyses has shown that both methods provide a wider range of solutions with greater flexibility for more general parameters. These findings add to the analytical understanding of nonlinear wave propagation and provide a useful framework for exploring similar nonlinear models. However, the present work has some limitations. The applied methods mainly generate particular classes of exact traveling wave solutions under specific assumptions. Therefore, more complex wave structures, such as rogue waves, multi-soliton solutions, and breather waves, are not obtained within the present framework. Moreover, the derived results depend on the adopted transformations and parameter constraints, which may limit the range of obtainable solution families. Future work could extend these methods to stochastic versions of the KK equation or higher-dimensional nonlinear systems. In addition, this work shows that the two approaches are applicable and effective in the study of complex nonlinear phenomena, and they are complementary to the mathematical tools when solving the NLEEs of physics and applied mathematics. Future research may also focus on rogue waves, multi-soliton interactions, breather solutions, and other higher-order nonlinear wave structures by employing alternative analytical techniques. Further, the stability analysis and interaction behavior of the obtained soliton solutions may be investigated numerically to further explore their physical significance and practical applications. Another promising direction is the extension of the present framework to fractional-order nonlinear models through operators such as the Atangana–Baleanu, Caputo, and conformable fractional derivatives. These formulations are much more crucial in describing memory dependent works, hereditary impacts, and nonlocal, nonlinear wave propagation phenomena happening in plasma physics, fluid dynamics, optical fibers, and engineering models.

Use of AI tools declaration

The author declares that he has not used Artificial Intelligence (AI) tools in the creation of this article.

Acknowledgments

The author is thankful to the Deanship of Graduate Studies and Scientific Research at the University of Bisha for supporting this work through the Fast-Track Research Support Program.

Conflict of interest

The author declares there is no conflict of interest.

References

1. E. Tadmor, A review of numerical methods for nonlinear partial differential equations, *Bull. Am. Math. Soc.*, **49** (2012), 507–554. https://doi.org/10.1090/S0273-0979-2012-01379-4
2. C. Qiao, X. Long, L. Yang, Y. Zhu, W. Cai, Calculation of a dynamical substitute for the real Earth–Moon system based on Hamiltonian analysis, *Astrophys. J.*, **991** (2025), 46. https://doi.org/10.3847/1538-4357/adf73a
3. M. Tanaka, The stability of solitary waves, *Phys. Fluids*, **29** (1986), 650–655. https://doi.org/10.1063/1.865459
4. Y. Bo, D. Tian, X. Liu, Y. Jin, Discrete maximum principle and energy stability of the compact difference scheme for two-dimensional Allen-Cahn equation, *J. Funct. Spaces*, **2022** (2022), 8522231. https://doi.org/10.1155/2022/8522231

5. A. Javid, A. R. Seadawy, N. Raza, Dual-wave of resonant nonlinear Schrodinger's dynamical equation with different nonlinearities, *Phys. Lett. A*, **407** (2021), 127446. https://doi.org/10.1016/j.physleta.2021.127446
6. J. S. Russell, *The Wave of Translation in the Oceans of Water, Air, and Ether*, Trübner & Co., 1885.
7. P. G. Drazin, R. S. Johnson, *Solitons: An Introduction*, Cambridge University Press, 1989.
8. N. Raza, A. Javid, Dynamics of optical solitons with radhakrishnan–kundu–lakshmanan model via two reliable integration schemes, *Optik*, **178** (2019), 557–566. https://doi.org/10.1016/j.ijleo.2018.09.133
9. I. S. Hamad, K. K. Ali, Investigation of brownian motion in stochastic Schrödinger wave equation using the modified generalized Riccati equation mapping method, *Opt. Quantum Electron.*, **56** (2024), 996. https://doi.org/10.1007/s11082-024-06865-y
10. D. Kumar, K. Hosseini, F. Samadani, The sine-gordon expansion method to look for the traveling wave solutions of the tzitzéica type equations in nonlinear optics, *Optik*, **149** (2017), 439–446. https://doi.org/10.1016/j.ijleo.2017.09.066
11. E. Az-Zo'bi, A. F. Al-Maaitah, M. A. Tashtoush, M. S. Osman, New generalised cubic-quintic-septic NLSE and its optical solitons, *Pramana*, **96** (2022), 184. https://doi.org/10.1007/s12043-022-02427-7
12. E. A. Az-Zo'bi, Q. M. Alomari, K. Afef, M. Inc, Dynamics of generalized time-fractional viscous-capillarity compressible fluid model, *Opt. Quantum Electron.*, **56** (2024), 629. https://doi.org/10.1007/s11082-023-06233-2
13. M. M. Miah, H. M. S. Ali, M. A. Akbar, A. M. Wazwaz, Some applications of the (g′/g, 1/g)-expansion method to find new exact solutions of NLEEs, *Eur. Phys. J. Plus*, **132** (2017), 252. https://doi.org/10.1140/epjp/i2017-11571-0
14. F. C. Lima, F. C. Simas, K. Z. Nobrega, A. R. Gomes, Boundary scattering in the $\phi 6$ model, *J. High Energy Phys.*, **2019** (2019), 147. https://doi.org/10.1007/JHEP10(2019)147
15. M. Khater, S. Anwar, K. U. Tariq, M. S. Mohamed, Some optical soliton solutions to the perturbed nonlinear Schrödinger equation by modified khater method, *AIP Adv.*, **11** (2021), 025130. https://doi.org/10.1063/5.0038671
16. S. Zhang, T. Xia, A generalized new auxiliary equation method and its applications to nonlinear partial differential equations, *Phys. Lett. A*, **363** (2007), 356–360. https://doi.org/10.1016/j.physleta.2006.11.035
17. J. Hietarinta, Hirota's bilinear method and soliton solutions, *Phys. AUC*, **15** (2005), 31–37.
18. N. Kadkhoda, H. Jafari, Analytical solutions of the Gerdjikov–Ivanov equation by using exp (- φ (ξ))-expansion method, *Optik*, **139** (2017), 72–76. https://doi.org/10.1016/j.ijleo.2017.03.078
19. S. Novikov, S. V. Manakov, L. P. Pitaevskii, V. E. Zakharov, *Theory of Solitons: The Inverse Scattering Method*, Springer Science & Business Media, 1984.
20. H. M. S. Ali, M. A. Habib, M. M. Miah, M. A. Akbar, A modification of the generalized Kudryashov method for the system of some nonlinear evolution equations, *J. Mech. Cont. Math. Sci.*, **14** (2019), 91–109. https://doi.org/10.26782/jmcms.2019.02.00007
21. A. M. Wazwaz, A sine-cosine method for handling nonlinear wave equations, *Math. Comput. Model.*, **40** (2004), 499–508. https://doi.org/10.1016/j.mcm.2003.12.010

22. H. Jafari, N. Kadkhoda, D. Baleanu, Fractional Lie group method of the time-fractional Boussinesq equation, *Nonlinear Dyn.*, **81** (2015), 1569–1574. https://doi.org/10.1007/s11071-015-2091-4

23. F. Tuffour, E. Akweittey, B. Barnes, I. K. Dontwi, W. Obeng-Denteh, K. F. Darkwah, The modified homogeneous balance method for finding solitons of the fractional Kaup-Kupershmidt equation, *Phys. Lett. A*, **584** (2026), 131603. https://doi.org/10.1016/j.physleta.2026.131603

24. R. M. Makwana, S. R. Khirsariya, On the solution of nonlinear fractional Kaup–Kupershmidt equations using a modified Adomian technique, *Bol. Soc. Mat. Mex.*, **32** (2026), 6. https://doi.org/10.1007/s40590-025-00837-2

25. M. V. Demina, N. A. Kudryshov, Point vortices and polynomials of the Sawada-Kotera and Kaup-Kupershmidt equations, *Regul. Chaotic Dyn.*, **16** (2011), 562–576. https://link.springer.com/article/10.1134/S1560354711060025

26. A. Akbulut, M. Kaplan, M. K. A. Kaabar, New conservation laws and exact solutions of the special case of the fifth-order KdV equation, *J. Ocean Eng. Sci.*, **7** (2022), 377–382. https://doi.org/10.1016/j.joes.2021.09.010

27. M. Inc, M. Miah, A. Chowdhury, S. Ali, A. Chowdhury, H. Rezazadeh, et al., New exact solutions for the Kaup-Kupershmidt equation, *AIMS Math.*, **5** (2020), 6726–6738. http://dx.doi.org/10.3934/math.2020432

28. N. Iqbal, H. Yasmin, A. Rezaiguia, J. Kafle, A. O. Almatroud, T. S. Hassan, Analysis of the fractional-order Kaup–Kupershmidt equation via novel transforms, *J. Math.*, **2021** (2021), 2567927. https://doi.org/10.1155/2021/2567927

29. J. Kim, C. H. Choi, S. J. Yeom, N. Eom, K. K. Kang, C. S. Lee, Directed assembly of Janus cylinders by controlling the solvent polarity, *Langmuir*, **33** (2017), 7503–7511. https://doi.org/10.1021/acs.langmuir.7b01252

30. A. Parker, On soliton solutions of the Kaup-Kupershmidt equation II: "Anomalous" N-soliton solutions, *Physica D*, **137** (2000), 34–48. https://doi.org/10.1016/S0167-2789(99)00167-0

31. D. J. Kaup, R. A. Van Gorder, The inverse scattering transform and squared eigenfunctions for the nondegenerate 3×3 operator and its soliton structure, *Inverse Probl.*, **26** (2010), 055005. https://doi.org/10.1088/0266-5611/26/5/055005

32. M. A. Abdou, A. A. Soliman, Modified extended tanh-function method and its application on nonlinear physical equations, *Phys. Lett. A*, **353** (2006), 487–492. https://doi.org/10.1016/j.physleta.2006.01.013

33. M. S. Alharthi, Extracting solitary solutions of the nonlinear Kaup–Kupershmidt equation by analytical method, *Open Phys.*, **21** (2023), 20230134. https://doi.org/10.1515/phys-2023-0134

34. H. O. Roshid, M. N. Alam, M. A. Akbar, Traveling wave solutions for fifth order $(1+1)$-dimensional Kaup-Kupershmidt equation with the help of $\exp(-\Phi)$-expansion method, *Walailak J. Sci. Tech.*, **12** (2015), 1063–1073.

35. S. Sahoo, S. S. Ray, M. A. Abdou, New exact solutions for time-fractional Kaup-Kupershmidt equation using improved (G'/G)-expansion and extended (G'/G)-expansion methods, *Alexandria Eng. J.*, **59** (2020), 3105–3110. https://doi.org/10.1016/j.aej.2020.06.043

36. Z. Z. Lan, Y. T. Gao, J. W. Yang, C. Q. Su, B. Q. Mao, Solitons, Bäcklund transformation and Lax pair for a (2 + 1)-dimensional Broer-Kaup-Kupershmidt system in the shallow water of uniform depth, *Commun. Nonlinear Sci. Numer. Simul.*, **44** (2017), 360–372. https://doi.org/10.1016/j.cnsns.2016.07.013
37. M. F. Alotaibi, N. Raza, M. H. Rafiq, A. Soltani, New solitary waves, bifurcation and chaotic patterns of Fokas system arising in monomode fiber communication system, *Alexandria Eng. J.*, **67** (2023), 583–595. https://doi.org/10.1016/j.aej.2022.12.069
38. H. Rezazadeh, New soliton solutions of the complex Ginzburg-Landau equation with Kerr law nonlinearity, *Optik*, **167** (2018), 218–227. https://doi.org/10.1016/j.ijleo.2018.04.026
39. M. Ozisik, A. Secer, M. Bayram, On solitary wave solutions for the extended nonlinear Schrödinger equation via the modified F-expansion method, *Opt. Quantum Electron.*, **55** (2023), 215. https://doi.org/10.1007/s11082-022-04476-z
40. T. A. Alrebdi, N. Raza, S. Arshed, F. H. Alkallas, A. H. Abdel-Aty, Soliton propagation and evolution in 1D quantum systems: a study of higher-order dispersion and nonlinear effects, *Open Phys.*, **24** (2026), 20250290. https://doi.org/10.1515/phys-2025-0290
41. S. S. Veni, M. M. Rajan, C. B. Tabi, T. C. Kofané, Propagation dynamics and modulation instability control in inhomogeneous nonlinear Schrödinger equation with two-photon absorption, *Chaos Solitons Fractals*, **202** (2026), 117605. https://doi.org/10.1016/j.chaos.2025.117605
42. D. Chou, I. Iqbal, H. U. Rehman, H. Ahmad, T. Radwan, Dynamics of low-pass electrical transmission lines: Lie symmetries, solitons, bifurcations, and modulation instability, *J. Nonlinear Math. Phys.*, 33 (2025). https://doi.org/10.1007/s44198-025-00356-8
43. A. Alleddawi, S. Momani, E. A. Az-Zo'bi, A novel higher-order dispersive extension of the generalized Hunter-Saxton model: Traveling-wave solutions, time-fractional impacts, and qualitative analysis, *Mod. Phys. Lett. B*, **40** (2026), 2650105. https://doi.org/10.1142/S0217984926501058
44. M. Eslami, H. Rezazadeh, The first integral method for Wu–Zhang system with conformable time-fractional derivative, *Calcolo*, **53** (2016), 475–485. https://doi.org/10.1007/s10092-015-0158-8
45. M. M. Al-Sawalha, S. Mukhtar, A. S. Alshehry, M. Alqudah, M. S. Aldhabani, Kink soliton phenomena of fractional conformable Kairat equations, *AIMS Math.*, **10** (2025), 2808–2828. https://doi.org/10.3934/math.2025131
46. D. Feng, K. Li, On exact traveling wave solutions for (1 + 1)-dimensional Kaup-Kupershmidt equation, *Appl. Math.*, **2** (2011), 752–756. https://doi.org/10.4236/am.2011.26100
47. M. Shakeel, S. Mohyud-Din, An alternative (G'/G)-expansion method with generalized Riccati equation: Application to fifth order (1 + 1)-dimensional Kaup-Kupershmidt equation, *Open J. Math. Model.*, **5** (2013), 173. https://doi.org/10.12966/ojmmo.09.04.2013

AIMS Press